

## Supporting Information

### Highly Conductive Ester-Based Solid Electrolyte Exhibiting Remarkable Stability for Safe, Sustainable, and High-Performance Lithium Metal Batteries

Yunfan Shao<sup>1</sup>, Wanlin Chen<sup>2</sup> and Cristina Iojoiu<sup>1,3,\*</sup>

<sup>1</sup>Univ. Grenoble Alpes, Univ. Savoie Mont Blanc, CNRS, Grenoble INP, LEPMI, 38000 Grenoble, France

<sup>2</sup> Department of Physical Chemistry II, Ruhr-Universität Bochum, 44801 Bochum, Germany

<sup>3</sup> Réseau sur le Stockage Electrochimique de l'Energie (RS2E), CNRS, FR3459, 80039 Amiens Cedex, France

Corresponding author e-mail: [Cristina.Iojoiu@grenoble-inp.fr](mailto:Cristina.Iojoiu@grenoble-inp.fr)

## Experimental

### **PBM and CPBM synthesis and characterization**

#### *Materials*

Dimethyl malonate was purchased from Janssen chemicals. 1,4-butanediol, divinyl sulfone (DVS) and tin(II) 2-ethylhexanoate ( $\text{Sn}(\text{Oct})_2$ ) was purchased from TCI. 1,8-Diazabicyclo[5.4.0]undec-7-ene (DBU) was purchased from Acros. Lithium bis(trifluoromethanesulfonyl)imide (LiTFSI) was purchased from Aldrich. Lithium bis(fluorosulfonyl)imide (LiFSI) was purchased from Carl Roth. All the reagents were used without purification.

#### *Synthesis of poly(butyl malonate) (PBM)*

200 mmol of dimethyl malonate, 200 mmol of 1,4-butanediol and 0.2 mmol of  $\text{Sn}(\text{Oct})_2$  introduced in a round flask equipped with magnetic stirring, air condenser and distillation apparatus. The mixture was heated to 120 °C for 12 h at ambient pressure and subsequently reduced pressure of 40 mbar for another 12 h. Side product methanol was removed by the distillation. The product was kept at vacuum of 0.1 mbar at 120 °C for another 12 h. The product is a yellowish viscous liquid. The polymer was used without further purification.

#### *Synthesis of CPBM/LiTFSI polymer electrolyte*

Crosslinked poly(butyl malonate) membranes were obtained by adding divinyl sulfone (DVS).

The molecular weight between the crosslinks  $M_c$  and the amount of crosslinker follows the following equation:

$$M_c = \frac{n_{BM}}{n_{DVS}} \times M_{BM}$$

where  $n_{BM}/n_{DVS}$  is the molar ratio between the structural units of BM (from poly(butyl malonate)) and the crosslinker divinyl sulfone,  $M_{BM}$  is the molar mass of the repeat unit of the polymer. Here, thanks to the

very efficient Michael addition reaction, we assume that all the DVS has been reacted to create a crosslinking point. The choice of the  $M_c$  value is critical in designing the crosslinked system, as the degree of crosslinking significantly influences the flexibility of the polymer chains and their mechanical behavior. If the  $M_c$  is too low, the crosslinked network becomes overly rigid, leading to reduced ionic conductivity and increased brittleness of the membrane. Conversely, the too high  $M_c$ , (i.e., low crosslinking), the mechanical strength of the membrane becomes poor. To achieve a sufficiently rigid and self-standing membrane (Figure S3), an optimal balance is achieved with a molecular weight ( $M_c$ ) of ~2000 g/mol, which was intentionally selected for this study.

In a typical formulation, 1 g of PBM polymer and 50  $\mu$ L of DVS (58.9 mg, 0.5 mmol) was mixed and was dissolved in 2 mL of acetonitrile. Desired amount of lithium salt and 10  $\mu$ L DBU (9.8 mg, 0.06 mmol) was dissolved in 1 mL of acetonitrile separately. The two solutions were then mixed in a PTFE petri dish and keep in an oven at 70 °C for 4 h. Then the membrane, with a thickness of 60  $\mu$ m was peeled off and dried under vacuum at 90 °C for 24 h.

### ***Characterization Methods***

$^1\text{H}$ ,  $^{13}\text{C}$ , and  $^{19}\text{F}$  NMR spectra were carried out with a Bruker Avance III HD 400 MHz NMR spectrometer and processed with the Bruker topspin software. The NMR samples were prepared with deuterated chloroform solvent.

Size exclusion chromatography (SEC) was conducted using a Waters 515 HPLC pump and 2414 RI detector with Styragel HR GPC column in THF solvent. The SEC was calibrated previously with standard polystyrene samples with different molecular weight.

ATR-FTIR spectra was carried out with a PerkinElmer Spectrum 3 spectrometer equipped with a Specac Quest ATR module. 32 scans were carried out with a range of 4000-450  $\text{cm}^{-1}$  for each sample.

Raman spectra was carried out with a Renishaw Virsa Raman spectrometer, equipped with 785 nm laser source and x50 LF objective lens. The laser power was 10 mW. The sample was prepared in an Ar-filled glove box, and seal with glass window to avoid contact with ambient atmosphere during the measurement.

Thermogravimetric analysis (TGA) of the samples was performed with a Mettler Toledo TGA1 system from 35 to 700 °C with rate of 10 °C  $\text{min}^{-1}$  in nitrogen atmosphere.

Differential scanning calorimetry (DSC) analysis of the samples was performed with a Mettler Toledo DSC3 system. The samples were sealed in an Ar-filled glovebox to avoid absorption of moisture. All the samples were heat to 125 °C with a rate of 10 °C  $\text{min}^{-1}$  to eliminate the thermal history and then scanned between 125 to -100 °C for 1 cycle. The  $T_g$  were measured on the second heating scanning.

SEM images of polymer membrane and lithium metal electrodes were collected with a ZEISS Ultra 55 SEM equipped with SE2 and Inlens detector. The cells after cycling were dissembled in an Ar-filled glovebox. The lithium samples were carefully transferred with the protection of Ar to limit the explosion in ambient atmosphere.

XPS spectra were obtained using a Thermo Scientific K-alpha spectrometer with a monochromated Al X-ray source (1486.6 eV ; spot size 400  $\mu$ m). The sample was prepared in an Ar-filled glovebox and transferred to the XPS with a vacuum transfer module avoiding explosion in air. The core level and the survey spectra were recorded with pass energies of 20 and 100 eV respectively. An electron flood gun was used to

compensate positive charge accumulation. The XPS spectra was process and deconvoluted by using the CasaXPS software.

### ***Molecular Dynamics***

Molecular Dynamics (MD) simulations of lithium salts (LiTFSI or LiFSI) dissolved in PBM polymer were performed. The simulation box is composed of 25 PBM chains of 15 repeating units and a varying number of lithium salts (15, 75, 150, 225), which corresponds to a O:Li ratio of 101.7, 20.3, 10.2, and 6.8. The generalized AMBER force field (GAFF) topologies were generated from the antechamber package from AmberTools25 to describe the PBM polymer, with the partial atomic charges fitted using the RESP method. The Li<sup>+</sup> cation was represented by the Aqvist force field,<sup>[1]</sup> the TFSI<sup>-</sup> anion by the CL&P model.<sup>[2]</sup>

All molecular dynamics simulations were performed using the GROMACS 2023.3 package. The LINCS algorithm was employed to constrain all bonds involving hydrogen atoms. Simulations were carried out in the NPT ensemble using the velocity-rescale thermostat and the C-rescale barostat. A global cutoff of 1.2 nm was applied for the Lennard-Jones interactions, while electrostatics were treated using the Particle Mesh Ewald (PME) method. The system was equilibrated following the protocol reported in ref.<sup>[3]</sup> After the energy minimization, the system is equilibrated following four sequential steps (2 ns each), at the following conditions: (i) 450 K and 1 bar, (ii) 450 K and 100 bar, (iii) 400 K and 100 bar, and (iv) 400 K and 1 bar. The system was then cooled and heated through three temperature cycles between 363 K and 400 K at 1 bar, 2 ns for each step. This was followed by an additional 10 ns equilibration at 363 K and 1 bar. Finally, a 100 ns production run was performed under the same conditions (363 K, 1 bar).

### ***Electrochemical characterizations***

All the electrochemical characterization was carried out with a Biologic VMP300 potentiostat. The data was process with Biologic EC-lab software.

Ionic conductivity of CPBM/LiTFSI electrolytes was performed with CR2032 coin cells with a configuration of stainless-steel (SS)|PE|SS at varied temperatures. Electrochemical impedance spectrometry (EIS) with frequency range of 7 MHz to 0.1 Hz was used to determine the electrolyte bulk resistance. The ionic conductivity was calculated with the following equation:

$$\sigma = \frac{L}{R_b \cdot A}$$

where L is the thickness, R<sub>b</sub> is the bulk resistance and A is the surface area of the electrolyte membrane.

Lithium transference number was measured with a modified Bruce-Vincent method<sup>[4]</sup> and Watanabe method<sup>[5]</sup>, with Li|SPE|Li cells at 80 °C. In modified Bruce-Vincent method, a chronoamperometry with 20 mV of bias voltage was applied to the cells for 8 h, EIS was recorded before and after the polarization. The T<sub>Li<sup>+</sup></sub> was calculated with the following equation:

$$T_{Li^+} = \frac{I_{ss}(\Delta V - I_0 R_0)}{I_0(\Delta V - I_{ss} R_{ss})}$$

$$I_0 = \frac{\Delta V}{R_{total}}$$

where, I<sub>0</sub>, R<sub>0</sub> and I<sub>ss</sub>, R<sub>ss</sub> represent the response of currents and interfacial resistances in initial and steady state, respectively, and ΔV is the bias voltage. Here the I<sub>0</sub> is determined by using the quotient of the ΔV and

total resistance (resistance at lowest frequency) rather than the measured value to eliminate the error introduced by the responds time of the device.

In Watanabe method, the lithium transference number is determined by the following equation:

$$T_{Li^+} = \frac{R_b}{\frac{\Delta V}{I_{ss}} - R_e}$$

where  $R_b$  and  $R_e$  corresponds to the electrolyte bulk resistance and interfacial resistance respectively.

Linear sweep voltammetry (LSV) and cyclic voltammetry (CV) were conducted with Li|PE|SS cells at 80 °C. The LSV was scanned from OCV to 0 V and 6 V separately with a scan rate of 0.1 mV s<sup>-1</sup>. CV was scanned from OCV to 4.5 V and then 0 V for 3 cycles.

Critical current density was carried out with symmetric Li|SPE|Li cells at 80 °C. Current scan experiment was applied from 0 to 2 mA with a scan rate of 0.1 μA s<sup>-1</sup>. 1<sup>st</sup> order derivation of the cell voltage vs. current density was calculated to examine the voltage transition.

Lithium stripping/plating experiments were conducted with symmetric Li|SPE|Li cells at 80 °C with various current densities. Chronopotentiometry was performed with desired current density for 4 h per stripping or plating. 15 min of rest at open-circuit state and a EIS was recorded between each chronopotentiometry process. Asymmetric Li|SPE|Cu cells was prepared with SPE sandwiched between Cu and Li foil electrodes. A precondition cycle of plating (2 mAh cm<sup>-2</sup>) and stripping until 1 V was applied. Followed by another 2 mAh cm<sup>-2</sup> of Li was plated on Cu as lithium reservoir. Subsequently, charge/discharge cycling of 0.1 mAh cm<sup>-2</sup> per cycle was repeated until the cell voltage exceeding 1 V. An EIS was recorded after each stripping/plating cycle.

Distribution relaxation times (DRT) of the EIS was calculated by using pyDRTtools from F. Ciucci et al.<sup>[6,7]</sup> EIS data was used from 220 kHz to 1 Hz avoiding the incomplete response at higher frequencies.

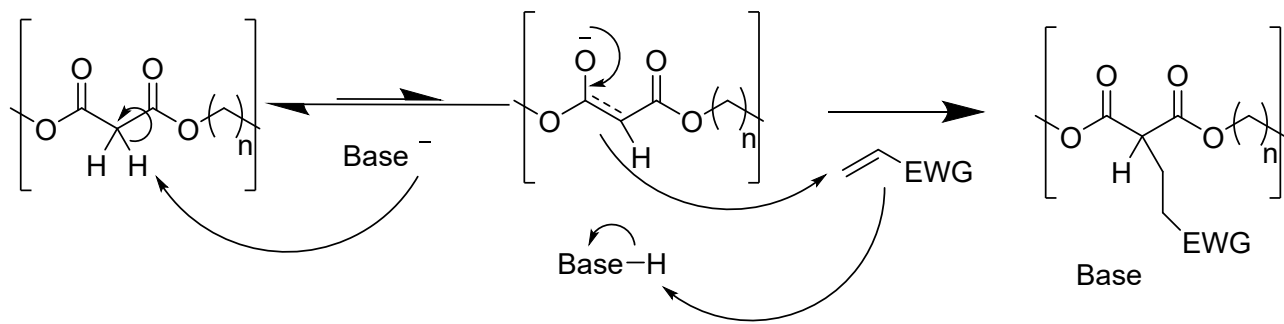
### *Electrode preparation*

Composite electrodes with active material LFP and LMFP were prepared with a mass ratio of active material: carbon black (TIMCAL super C65): PVdF (solef 6020)= 8:1:1. The active materials, carbon black was first mixed in a mortar, then the PVdF was added in a form of 5 wt.% solution in N-methyl-pyrrolidone. The slurry was then homogenized by using a Hauschild Speedmixer for 10 min at 5000 rpm. The electrode was casted by doctor blading the slurry on carbon coated Al foil, and dry at 80°C for 12 h. The electrode was then cut in discs of 12 mm diameter, dried under vacuum at 80 °C and kept in an Ar-filled gloved box before use. Typical mass loading of the active materials is ~ 3mg cm<sup>-2</sup>, with a coating thickness of 16-20 μm.

### *Battery Assembling and Testing*

Lithium metal battery cells are assembled in an argon-filled glove box. A thin layer of PBM/Li salt mixture (~10 mg cm<sup>-2</sup>) was first spread on the positive electrodes to fill the porosity in the electrodes before use. The CPBM/LiTFSI or CPBM/LiFSI membrane was then sandwiched between the positive electrode and lithium foil. The cells are sealed in form of CR2032-type coin cells or single-layered pouch cells.

After assemble, the cells were moved to an 80° C oven and rested for 12 h before electrochemical tests. Galvanostatic charge/discharge was applied for both LFP and LMFP cells, with a voltage limitation between 2.5 to 3.9 V for LFP cells and 2.5 to 4.4 V for LMFP cells.



Scheme S1. Mechanism of Michael addition for PBM modification.

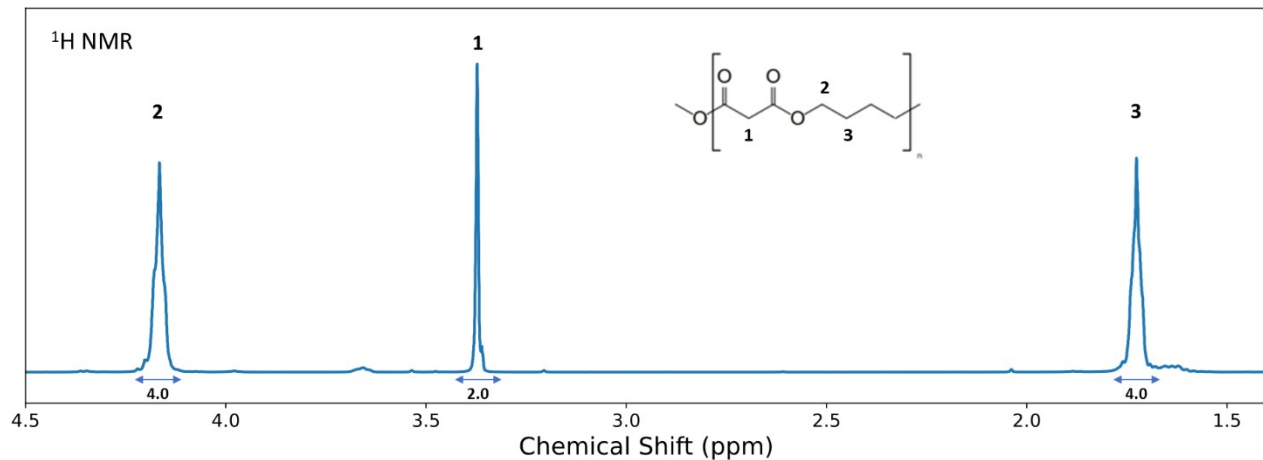


Figure S1.  $^1\text{H}$  NMR spectrum of PBM polymer.

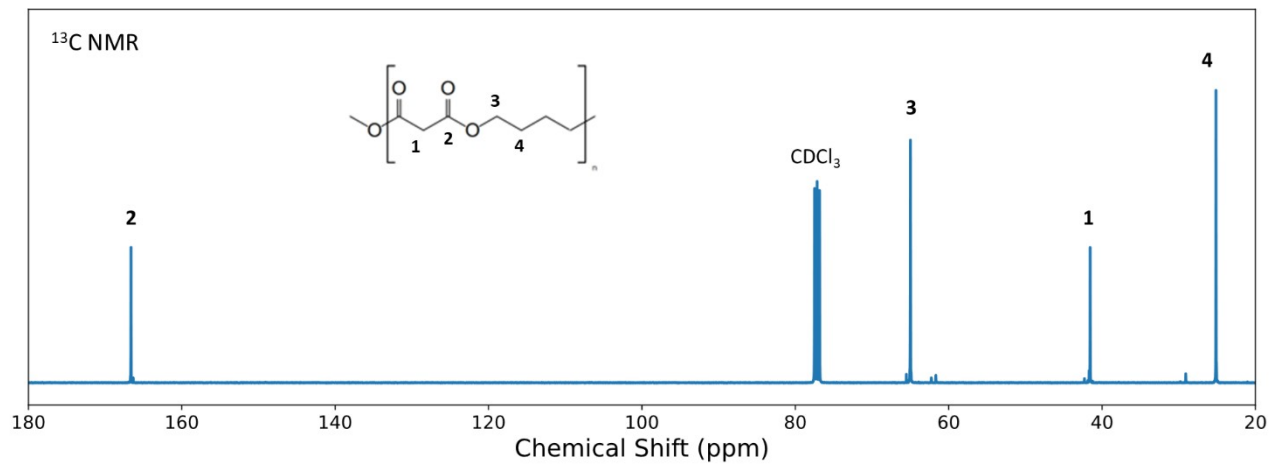


Figure S2. Composite pulse-decoupled <sup>13</sup>C NMR spectrum of PBM polymer.

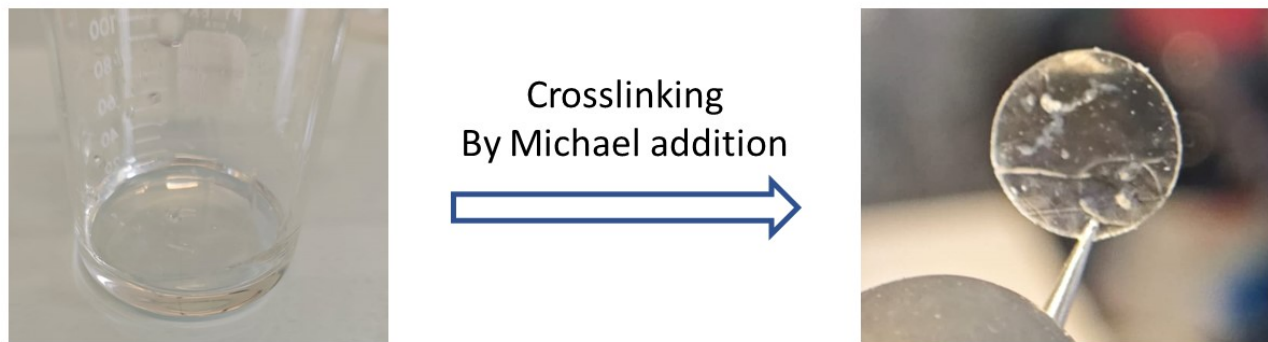


Figure S3. Images of PBM and CPBM polymers.

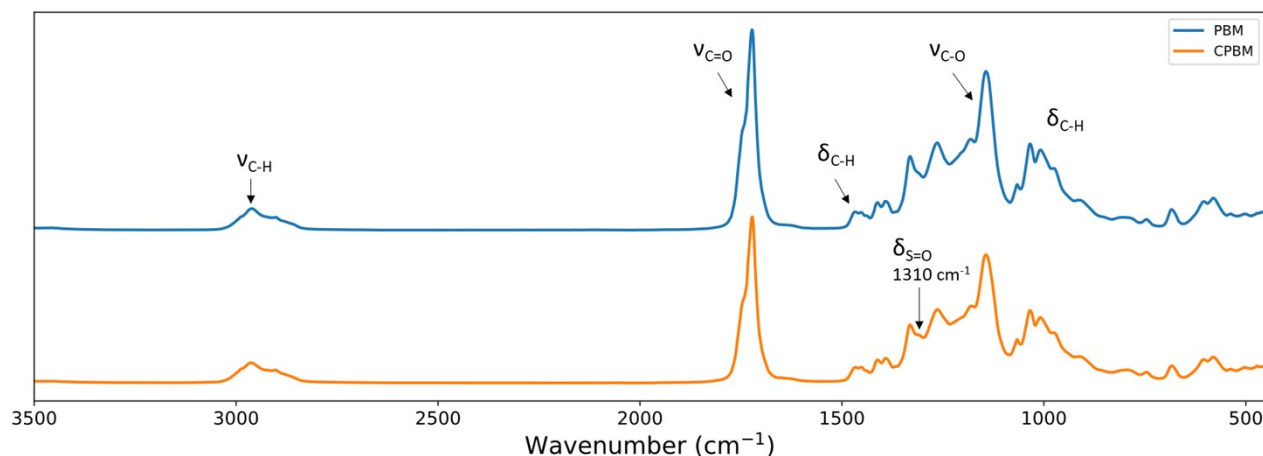


Figure S4. FT-IR spectra of PBM and CPBM polymers.

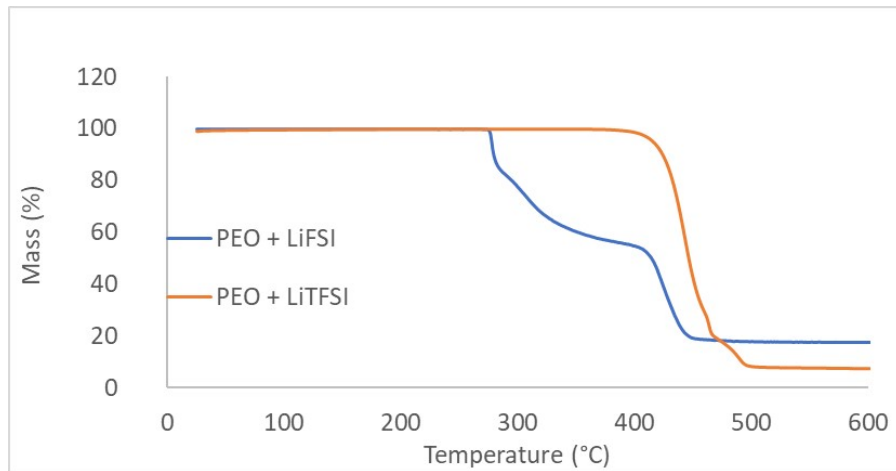


Figure S5. Thermogram of the PEO SPEs (O/Li = 28)

Table S1. Molecular weights of PBM polymer from SEC results.

$M_n$ (g mol $^{-1}$ )	$M_w$ (g mol $^{-1}$ )	$M_p$ (g mol $^{-1}$ )	PDI
12370	25810	18750	2.08

Table S2. Fitted VTF parameters for the ionic conductivity of CPBM-based SPEs.

	O:Li	$\sigma_0$ (S cm $^{-1}$ K $^{0.5}$ )	$T_0$ (K)	$E_a$ (kJ mol $^{-1}$ )	$E_a$ (eV)
CPBM/LiTFSI	28	5.59	201	9.57	0.099
CPBM/LiFSI	28	6.87	204	10.28	0.106

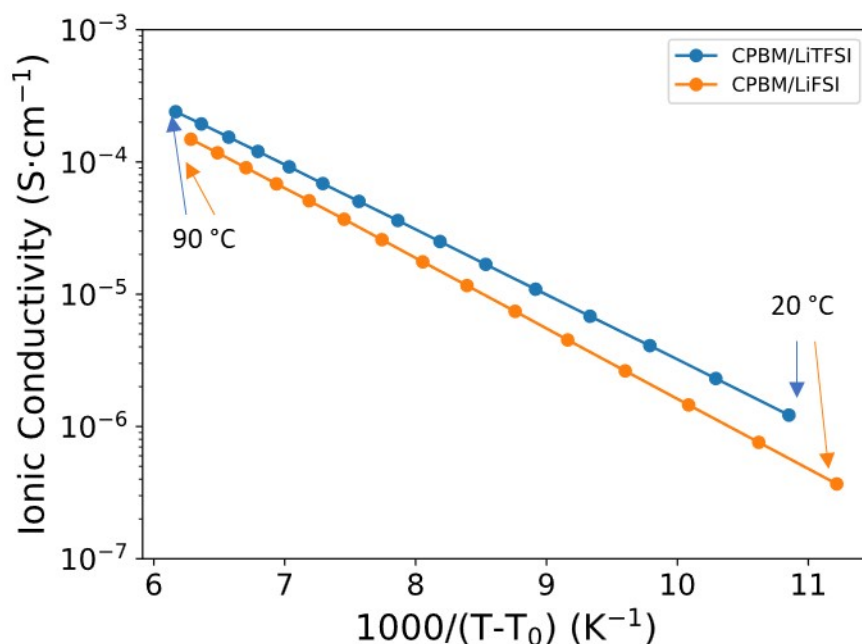


Figure S6. Ionic conductivities of SPEs with different salts as a function of  $1000/(T-T_0)$ .

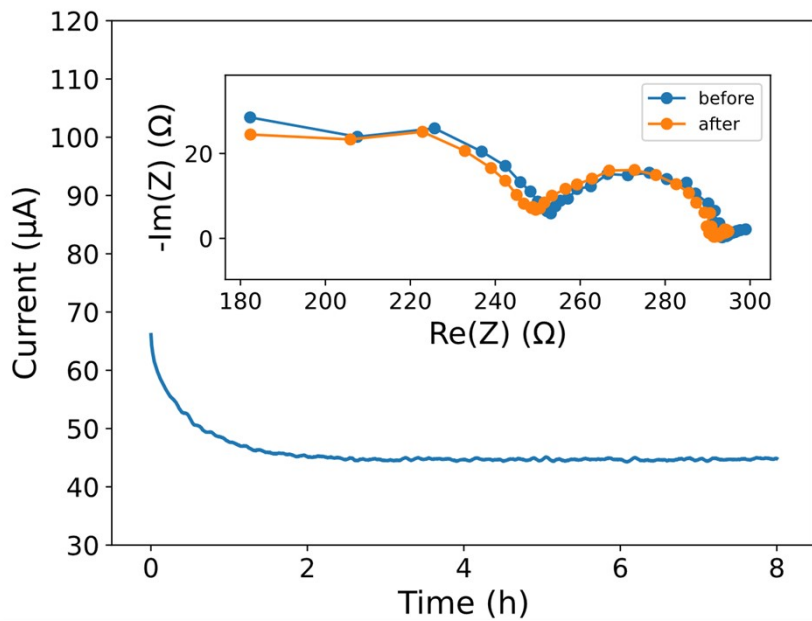


Figure S7. Chronoamperometry experiments conducted  $\text{Li}|\text{CPBM-LiTFSI}|\text{Li}$  cells with a bias voltage of 20 mv, with corresponding EIS spectra before and after the chronoamperometry experiments.

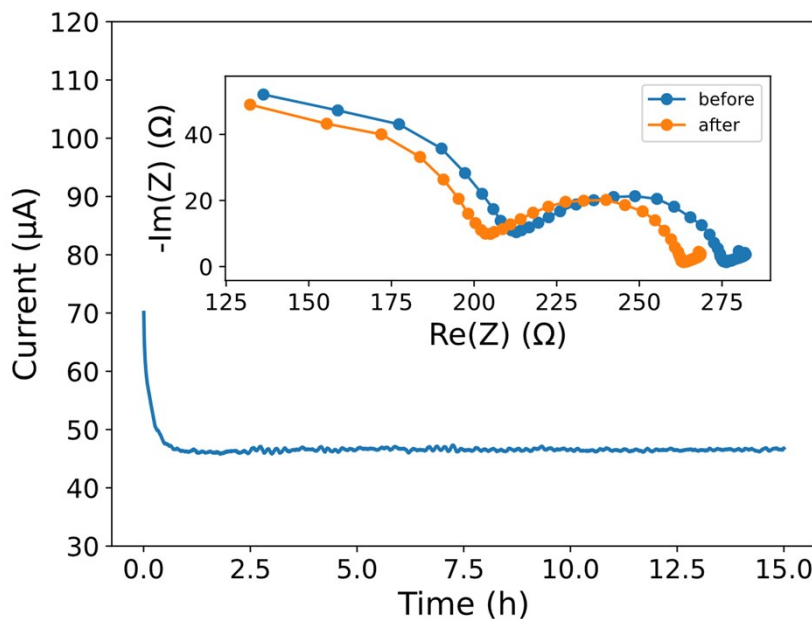


Figure S8. Chronoamperometry experiments conducted  $\text{Li}|\text{CPBM-LiFSI}|\text{Li}$  cells with a bias voltage of 20 mv, with corresponding EIS spectra before and after the chronoamperometry experiments.

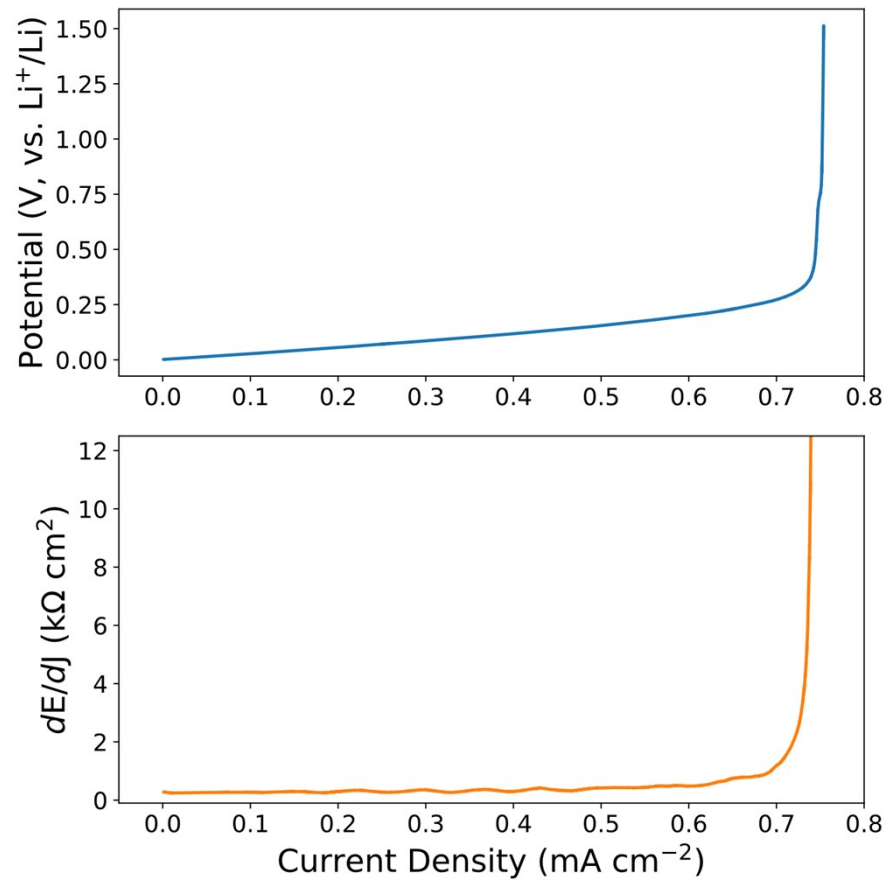


Figure S9. Determination of critical current density of the CPBM-LiTFSI SPE. Top: Current scan of a  $\text{Li}|\text{CPBM-LiTFSI}|\text{Li}$  cell at 80 °C, from 0 to 1 mA, with a rate of 0.1  $\mu\text{A s}^{-1}$ . Below: 1<sup>st</sup> order derivative of potential.

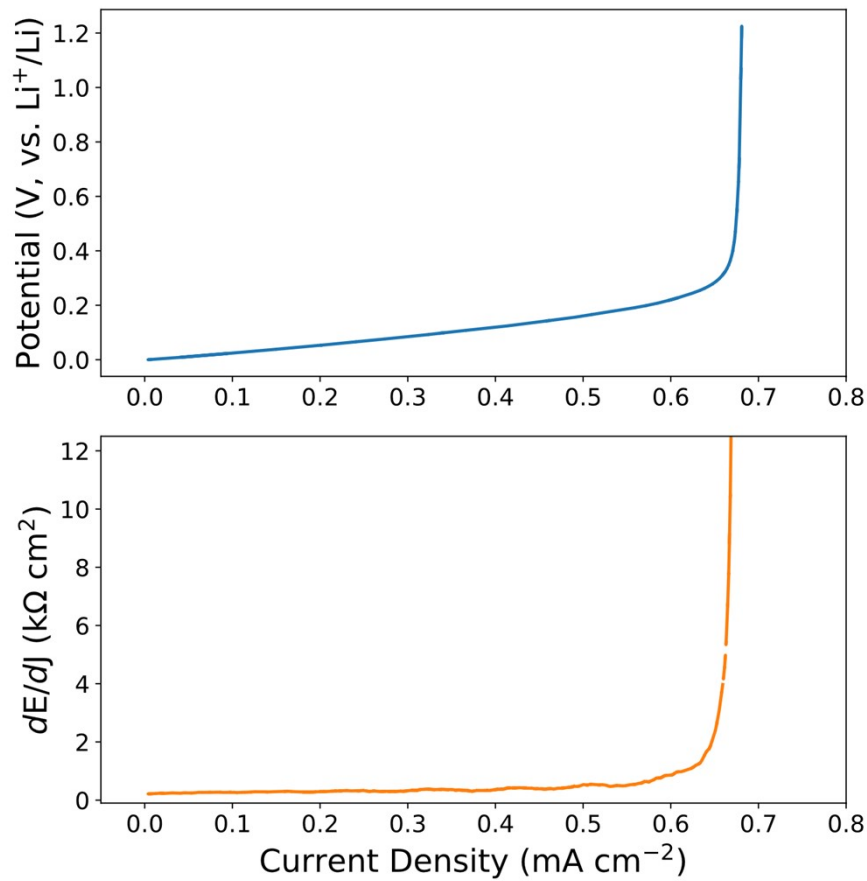


Figure S10. Determination of critical current density of the CPBM-LiFSI SPE. Top: Current scan of a Li|CPBM-LiFSI|Li cell at 80 °C, from 0 to 1 mA, with a rate of 0.1  $\mu\text{A s}^{-1}$ . Below: 1<sup>st</sup> order derivative of potential.

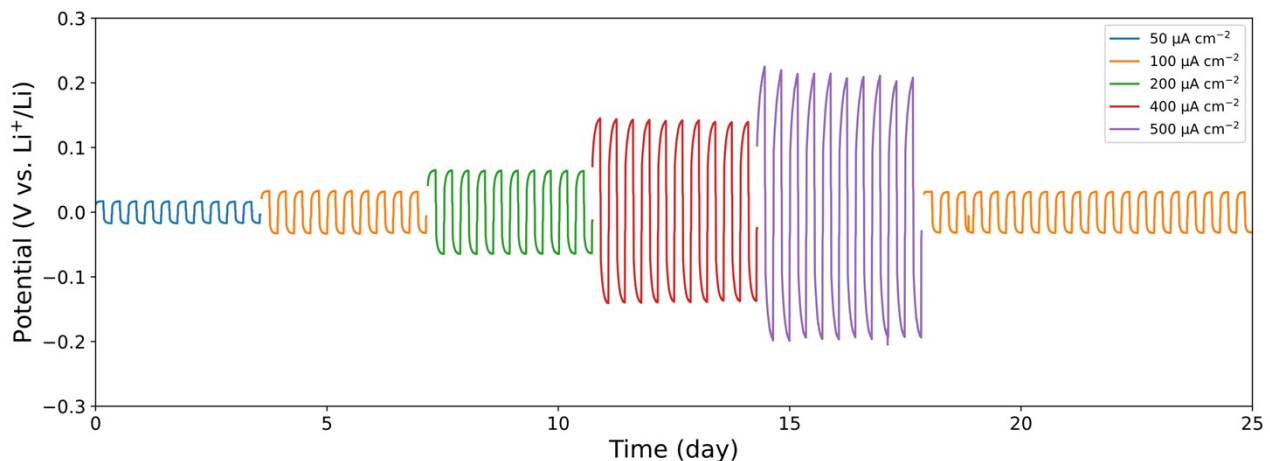


Figure S11. Lithium stripping/plating experiments of the Li|CPBM-LiTFSI|Li cells at 80 °C with varied current densities.

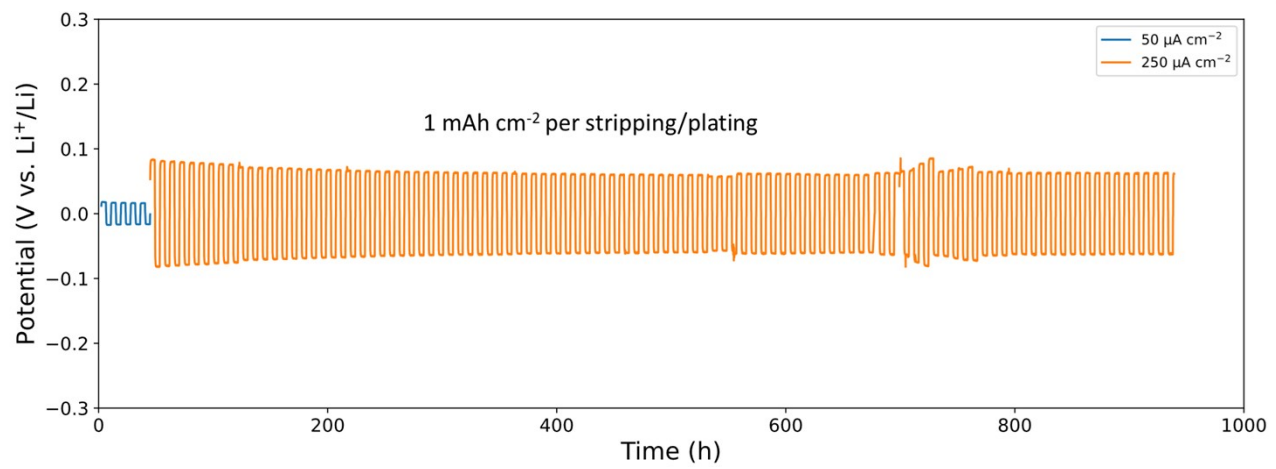


Figure S12. Lithium stripping/plating experiments of the Li|CPBM-LiTFSI|Li cells at 80 °C.

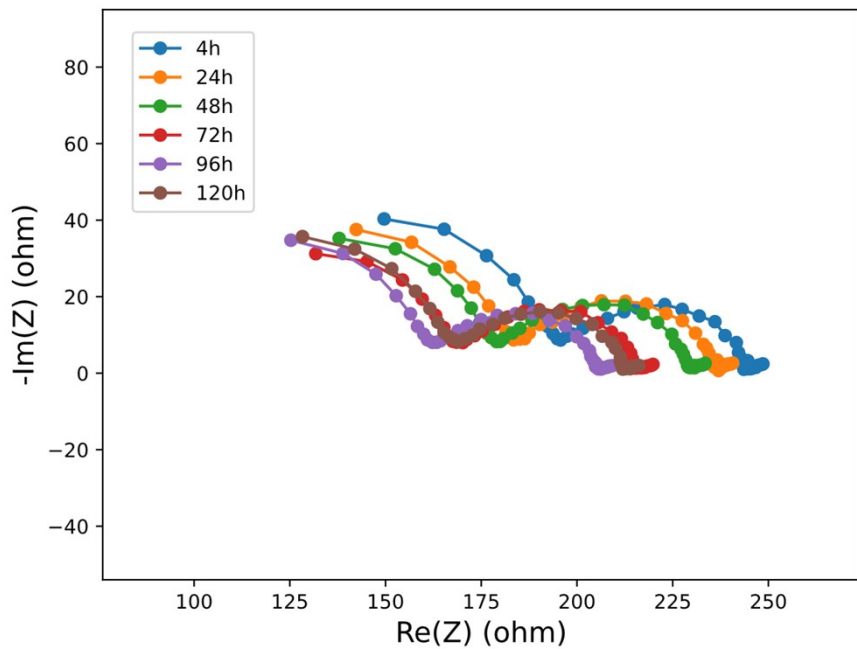


Figure S13. EIS spectra of the Li|CPBM-LiTFSI|Li cells recorded during the Li stripping/plating experiments.

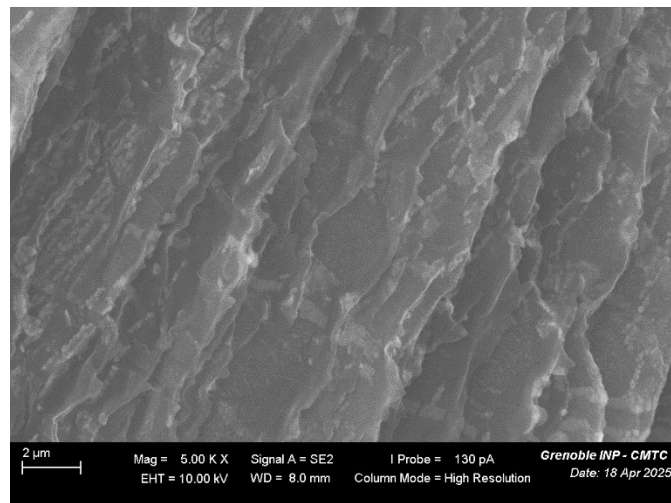


Figure S14. SEM image of lithium metal electrode in Li|CPBM/LiTFSI|Li cells after 900 h of lithium stripping/plating experiments.

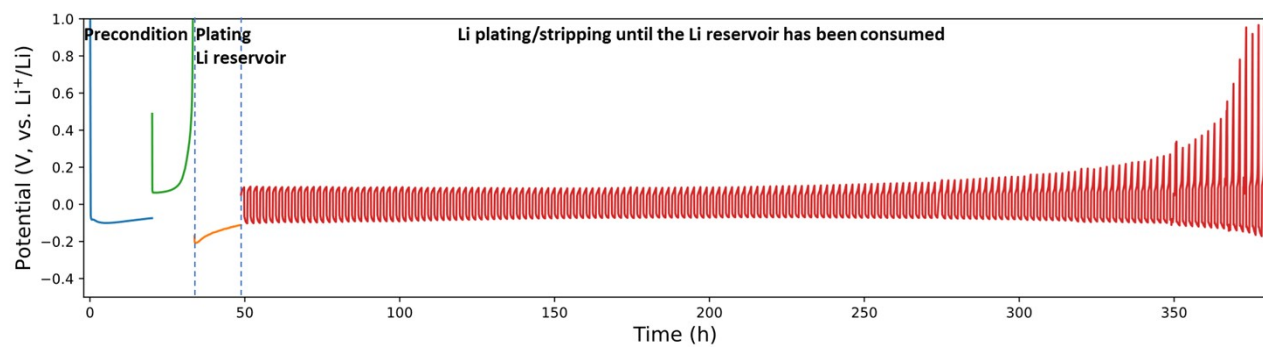
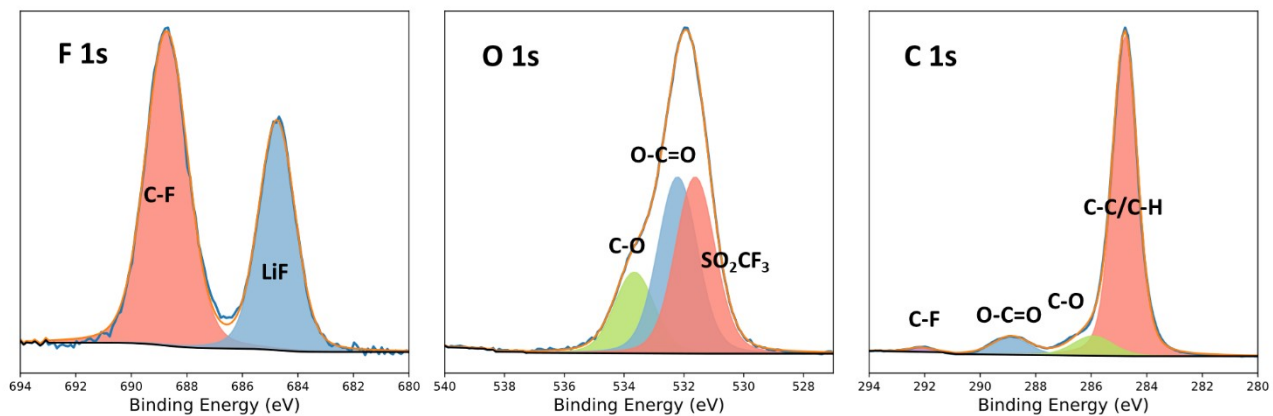


Figure S15. Lithium stripping/plating experiments of the Li|CPBM/LiTFSI|Cu cells at 80 °C for CE determination.

### CPBM/LiTFSI Pristine



### CPBM/LiTFSI After Cycling

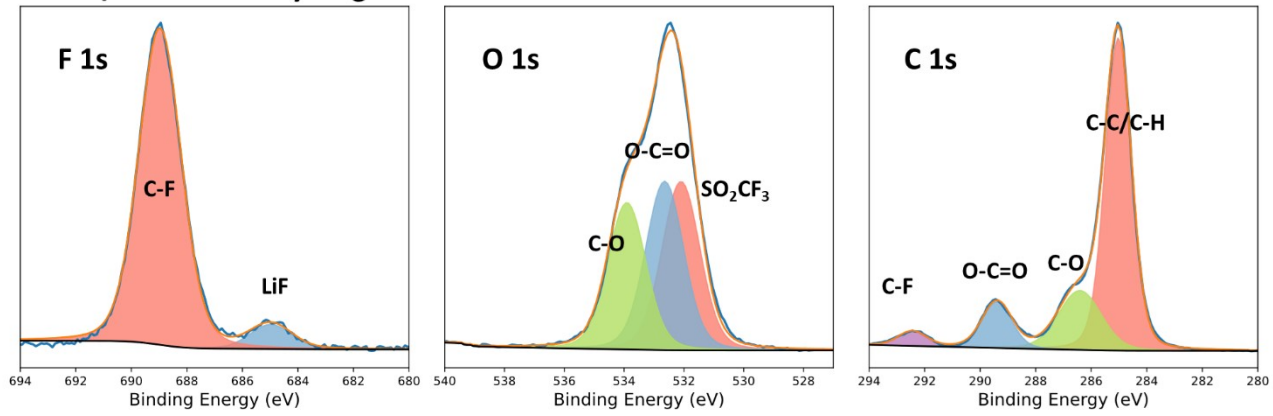


Figure S16. XPS spectra of CPBM/LiTFSI SPE before and after cycling in Li|CPBM/LiTFSI|Li cells.

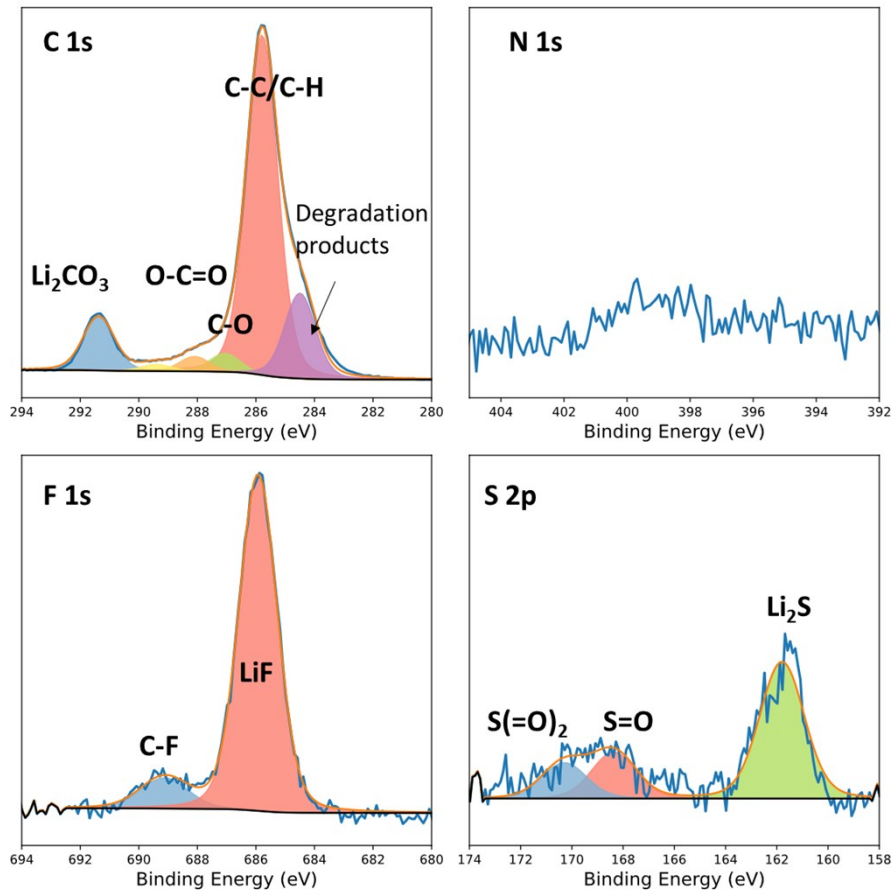


Figure S17. XPS spectra of lithium electrode after cycling in Li|CPBM/LiTFSI|Li cells.

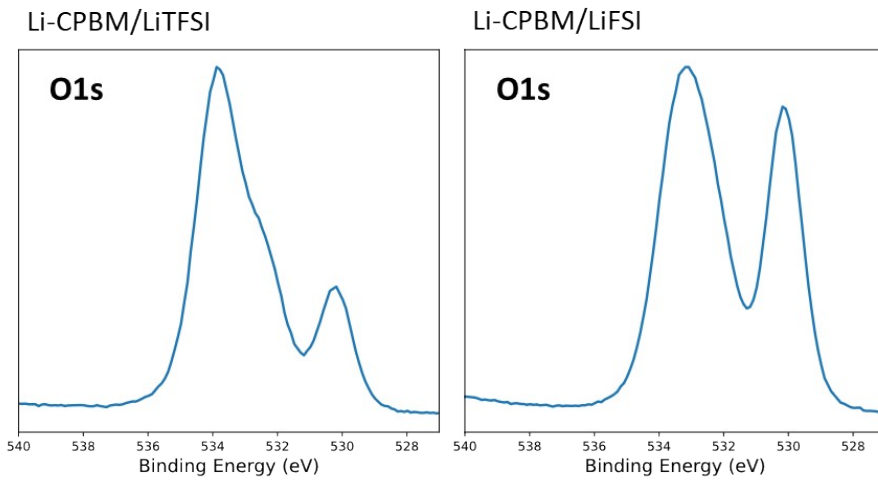


Figure S18. XPS O 1s spectra of lithium after cycling with CPBM electrolytes with different salts. Left: CPBM/LiTFSI right: CPBM/LiFSI.

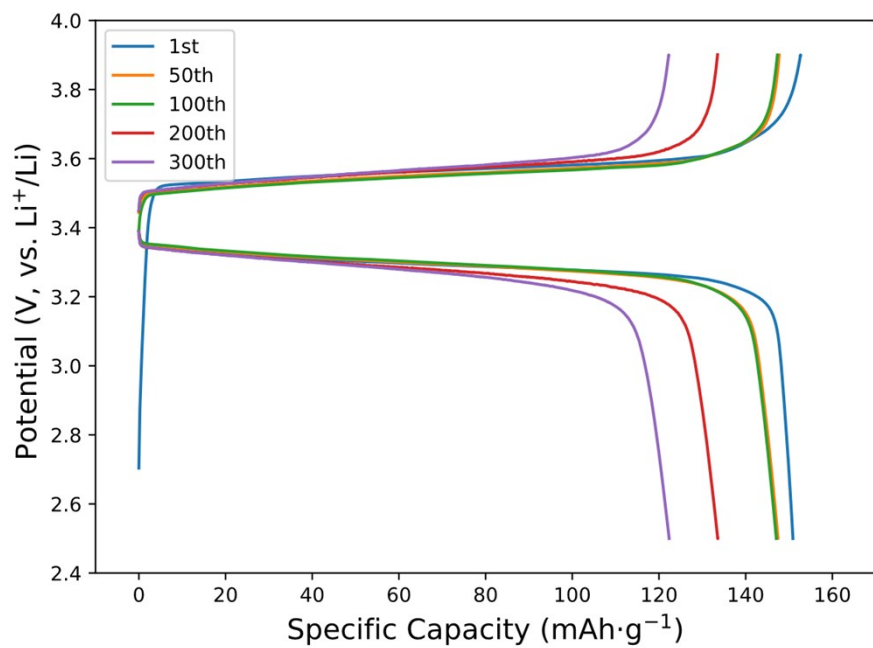


Figure S19. Selected dis-/charge profiles for Li|CPBM/LiTFSI|LFP cells at 80 °C.

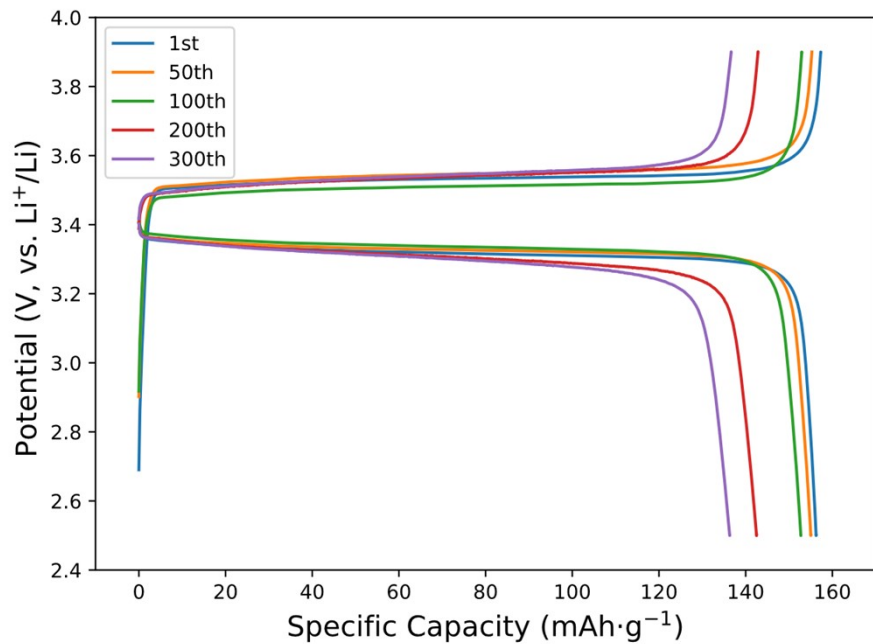


Figure S20. Selected dis-/charge profiles for Li|CPBM/LiFSI|LFP cells at 80 °C.

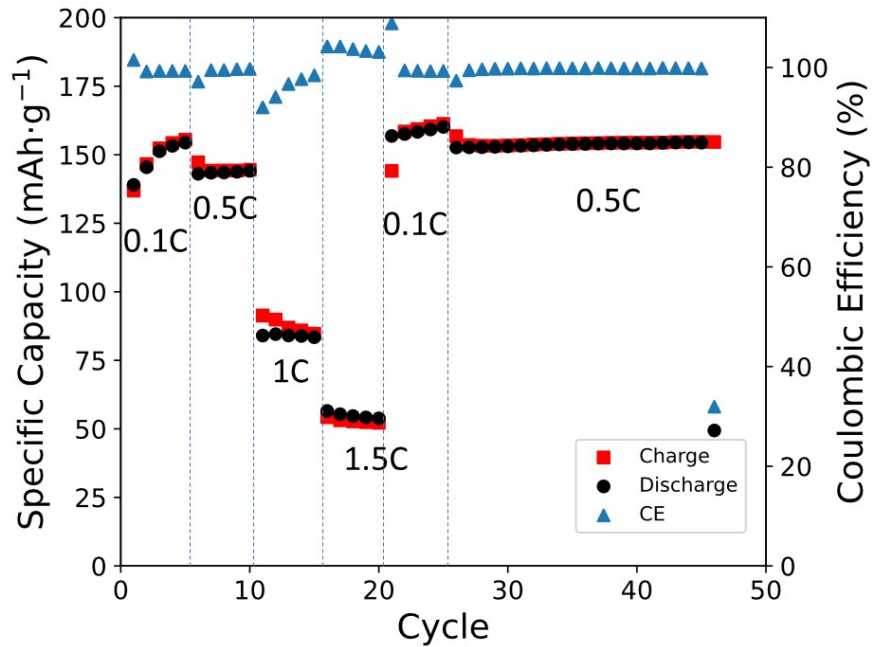


Figure S21. C-rate test for Li|CPBM/LiFSI|LFP cells at 80 °C.

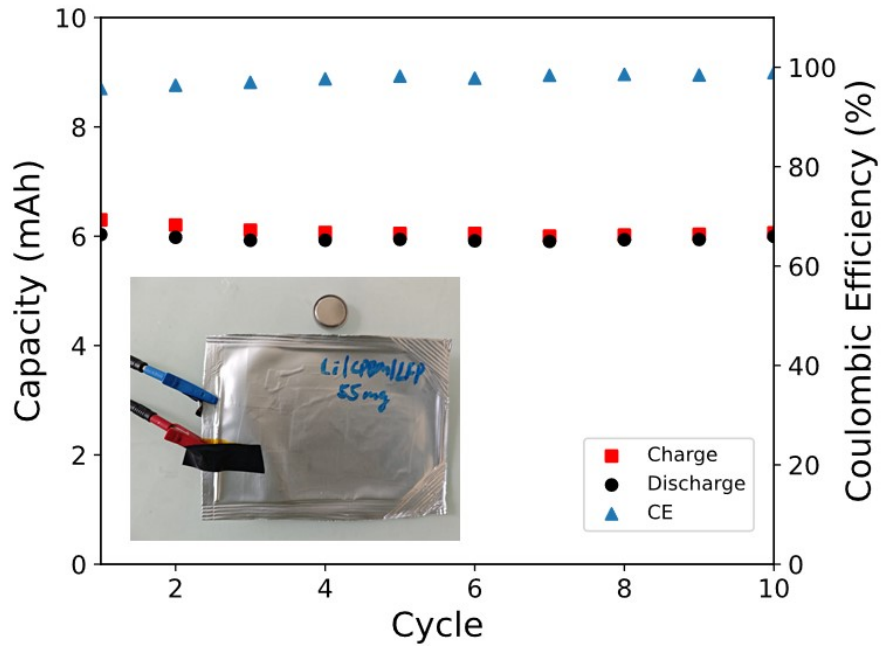


Figure S22. Image and cycling performance of prototype pouch cell.

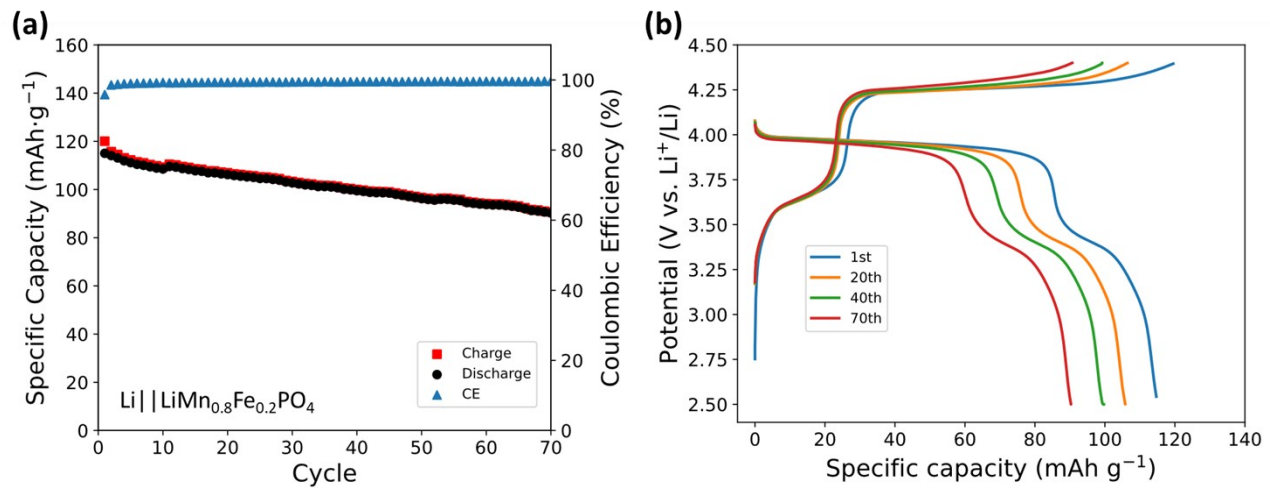


Figure S23. (a) Cycling performance of LMB cells with Mn-rich  $\text{LiMn}_{0.8}\text{Fe}_{0.2}\text{PO}_4$ . (b) corresponding dis-/charge profiles.

## References

- [1] J. Åqvist, *J. Phys. Chem.* **1990**, *94*, 8021.
- [2] J. N. Canongia Lopes, J. Deschamps, A. A. H. Pádua, *J. Phys. Chem. B* **2004**, *108*, 2038.
- [3] X. Yu, Z. J. Hoffman, J. Lee, C. Fang, L. A. Gido, V. Patel, H. B. Eitouni, R. Wang, N. P. Balsara, *ACS Energy Lett.* **2022**, *7*, 3791.
- [4] P. G. Bruce, C. A. Vincent, *J. Electroanal. Chem. Interfacial Electrochem.* **1987**, *225*, 1.
- [5] M. Watanabe, S. Nagano, K. Sanui, N. Ogata, *Solid State Ion.* **1988**, *28–30*, 911.
- [6] T. H. Wan, M. Saccoccio, C. Chen, F. Ciucci, *Electrochimica Acta* **2015**, *184*, 483.
- [7] A. Maradesa, B. Py, T. H. Wan, M. B. Effat, F. Ciucci, *J. Electrochem. Soc.* **2023**, *170*, 030502.